SHORT REPORT

VPS53 mutations cause progressive cerebello-cerebral atrophy type 2 (PCCA2)

Miora Feinstein,[1] Hagit Flusser,[2] Tally Lerman-Sagie,[3] Bruria Ben-Zeev,[4] Dorit Lev,[3] Orly Agamy,[1] Idan Cohen,[1] Rotem Kadir,[1] Sara Sivan,[1] Esther Leshinsky-Silver,[3] Barak Markus,[1] Ohad S Birk[1,5]

[1]Morris Kahn Laboratory of Human Genetics at the National Institute of Biotechnology in the Negev and Faculty of Health Sciences, Ben Gurion University, Beer Sheva, Israel
[2]Zussman Child Development Center, Soroka Medical Center, Faculty of Health Sciences, Ben Gurion University of the Negev, Beer Sheva, Israel
[3]Pediatric Neurology Unit, Institute of Medical Genetics, Wolfson Medical Center, Holon, Israel
[4]Pediatric Neurology Unit, Sheba Medical Center, Ramat-Gan, Israel
[5]Genetics Institute, Soroka Medical Center, Ben-Gurion University of the Negev, Beer Sheva, Israel

Correspondence to
Dr Ohad S Birk,
Genetics Institute, Soroka Medical Center, Beer-Sheva 84101, Israel;
obirk@bgu.ac.il

MF, HF, TL-S, BB-Z, DL and OA contributed equally.

ABSTRACT

Background Progressive cerebello-cerebral atrophy (PCCA) leading to profound mental retardation, progressive microcephaly, spasticity and early onset epilepsy, was diagnosed in four non-consanguineous apparently unrelated families of Jewish Moroccan ancestry. Common founder mutation(s) were assumed.
Methods Genome-wide linkage analysis and whole exome sequencing were done, followed by realtime PCR and immunofluorescent microscopy.
Results Genome-wide linkage analysis mapped the disease-associated gene to 0.5 Mb on chromosome 17p13.3. Whole exome sequencing identified only two mutations within this locus, which were common to the affected individuals: compound heterozygous mutations in *VPS53*, segregating as expected for autosomal recessive heredity within all four families, and common in Moroccan Jews (∼1:37 carrier rate). The Golgi-associated retrograde protein (GARP) complex is involved in the retrograde pathway recycling endocytic vesicles to Golgi; c.2084A>G and c.1556+5G>A *VPS53* founder mutations are predicted to affect the C-terminal domain of VPS53, known to be critical to its role as part of this complex. Immunofluorescent microscopy demonstrated swollen and abnormally numerous CD63 positive vesicular bodies, likely intermediate recycling/late endosomes, in fibroblasts of affected individuals.
Conclusions Autosomal recessive PCCA type 2 is caused by *VPS53* mutations.

INTRODUCTION

Progressive cerebello-cerebral atrophy (PCCA) caused by *SEPSECS* (MIM 613009) mutations was previously reported in Jews of Moroccan ancestry.[1][2] The phenotype in those families was distinct from pontocerebellar hypoplasias mainly due to the postnatal onset, lack of choreoathetosis (characteristic of Pontocerebellar Hypoplasia type 2 (MIM 277470)), and lack of pontine involvement on neuroimaging.[1][2] However, *SEPSECS* mutations were not found in similar patients from additional families of Jewish Moroccan origin, suggesting genetic heterogeneity of the phenotype in this cohort.[2] We now set out to identify the molecular basis of PCCA in those families.

MATERIAL AND METHODS
Linkage analysis
DNA samples were obtained following approval of the Soroka Medical Center institutional review board and informed consent. Genome-wide linkage analysis was done using Affymetrix 10 K single nucleotide polymorphism (SNP) arrays and Affymetrix GeneChip Human Mapping 500 K Set Nsp microarrays as previously described.[2]

Whole exome sequencing and data analysis
Whole exome sequencing was performed as previously described.[3] After filtering for known variants (SNP database (http://www.ncbi.nlm.nih.gov/projects/SNP), Seattle, WA, (http://evs.gs.washington.edu/EVS), accessed December 2011), sequence variants that were not annotated in any of the dbSNP or 1000 genomes databases were prioritised for further analysis.

Restriction analysis of the two *VPS53* mutations
PCR primers were designed (New England Biolabs NEBcutter) generating a recognition site for PvuII that is abolished by the c.2084A>G mutation (Primers: AAAAAATGCCTGATACTACGTCCATCTCAGC, TTCATGGAGATACGTGGAACC; wild-type allele restriction products 159 and 30 bp, versus uncut 189 bp for the mutant allele). For the c.1556+5G>A mutation, PCR primers were designed with a reverse primer sequence abrogating a second recognition site for TfiI. The remaining recognition site exists only in the mutated sequence. (Primers: TCTACTACAAGAAGTGCATGGTG, CAGAGTGGATTTCCTTAAGGTTC; mutant allele restriction products 171 and 33 bp, vs uncut 204 bp for the wild-type allele).

Realtime PCR studies
Epstein–Barr virus (EBV)-transformed lymphoblastoid cell lines were generated as previously described.[2] RNA was extracted from cultured cells (RNeasy Mini Kit, QIAGEN), and cDNA was reverse transcribed (Verso RT-PCR kits, TAMAR). Relative mRNA levels of *VPS53* were measured by quantitative RT-PCR using primer pairs designed to amplify different segments of the *VPS53* tanscript: primers amplifying exons 15–16: TCTGTAACATCCTGAGCACG and GTGTCCATCTCTCCAGTCAGA; primers amplifying exons 19–20: forward primer CATGGTGGGAGCAGAACA (for wild-type transcript) or CATGGTGGGAGCAGAACG (for c.2084A>G mutated transcript) and reverse primer TGCCTTTGACAACGATCTTG (for both). Each sample was analysed in triplicate. Results were normalised to glyceraldehyde 3-phosphate dehydrogenase (GAPDH) mRNA levels as previously described.[4]

Immunofluoresecnce microscopy studies of human fibroblasts

Fibroblast cell lines were isolated from skin biopsies of two affected individuals (D3 and D11, figure 1A) and unaffected controls. Immunostaining was performed with anti-CD63 antibodies (CBL553, Chemicon Millipore) as previously described.[4] Visualisation was done using an Olympus confocal microscope (×60 objective). Excitation was performed with a 488 nm (for EGFP) and 504 nm (for DAPI) laser and filtered accordingly. All confocal images were recorded under identical conditions. Quantification of number and volume of vesicles in fibroblasts was done using Volocity image analysis software (Impovision, Waltham, Massachusetts, USA) as previously described.[5]

RESULTS

Disease phenotype

Ten patients of four apparently unrelated non-consanguineous Jewish Moroccan non-SEPSECS PCCA families were studied
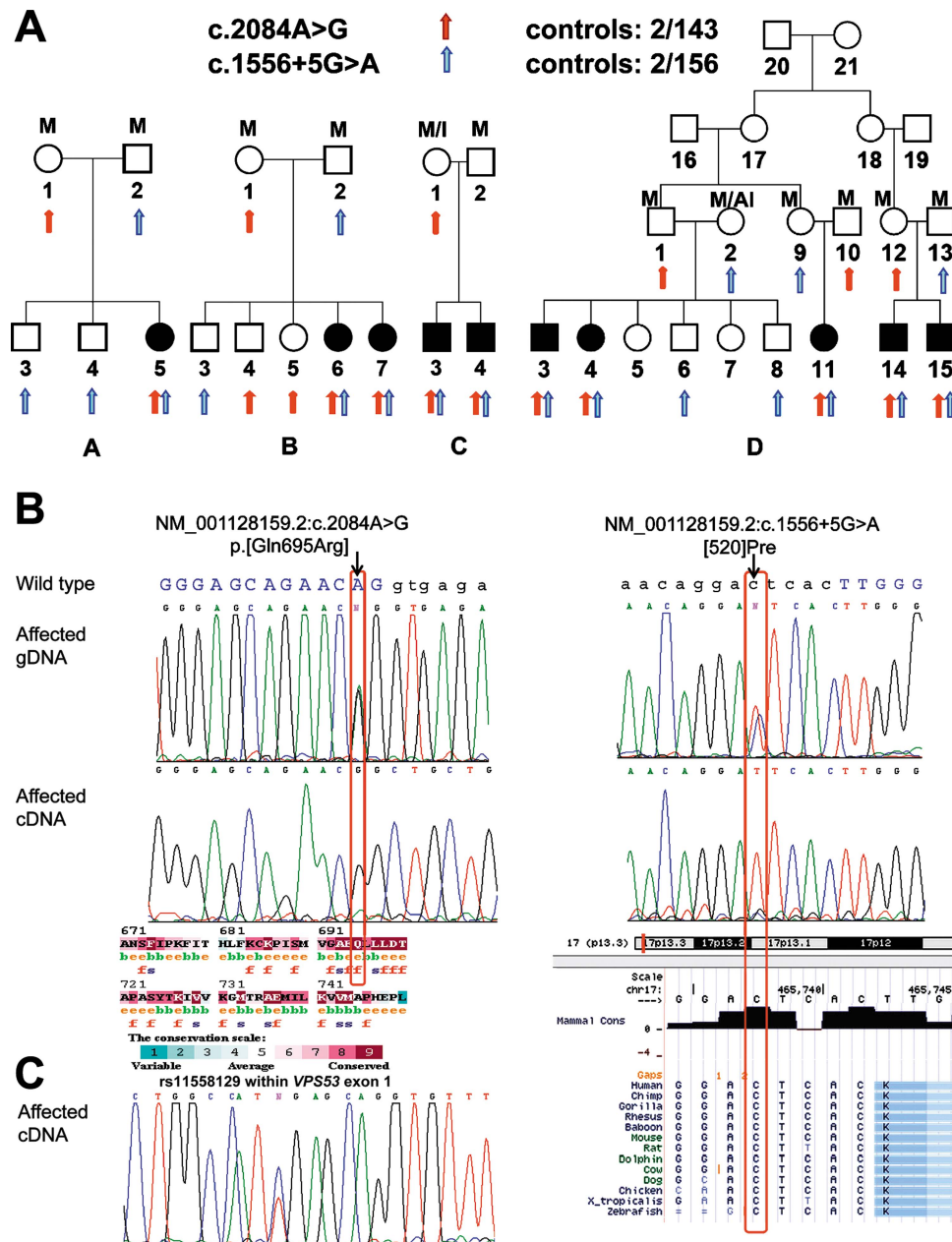

Figure 1 Pedigrees of studied kindred and the VPS53 mutations. (A) The four Jewish families studied (Families A, B, C and D). M = Moroccan, Al = Algerian, I = Iraqi. (B) The VPS53 c.2084A>G and c.1556+5G>A mutations: gDNA and cDNA sequences are shown for an affected individual that is compound heterozygous for both mutations. Note that in the cDNA sequence, the c.2084A>G mutation appears in an allegedly homozygous state, with no evident representation of transcripts of the second allele bearing the second mutation, c.1556+5G>A. The c.1556+5G>A mutation is also seemingly homozygous in the patient's cDNA, as it is an intronic mutation and the reaction was planned in a way that no fragment could be amplified from the wild-type allele. Arrows indicate mutations positions. Capital blue letters indicate exonic regions, whereas small black letters represent intronic ones. The premature stop codon arising from the c.1556+5G>A mutation is marked as 'Pre'. For each of the mutations, conservation is shown: ConSeq amino acid conservation for c.2084A>G (e, an exposed residue according to the neural-network algorithm; f, a predicted functional residue that is highly conserved and exposed), UCSC presentation of nucleotide conservation for c.1556+5G>A. (C) cDNA sequence of rs11558129 within exon 1 of VPS53 in an affected individual, demonstrating the existence of two alleles.

(figure 1A). Pregnancy and delivery were normal in all affected individuals. Head circumference was normal throughout pregnancy (per ultrasound) and at birth. Psychomotor development was initially normal, but irritability and mild hypotonia were evident in most patients during the first months of life. As of 3–5 months, psychomotor retardation became evident, accompanied by deceleration of head growth reaching less than 3rd percentile by 18 months. All patients had progressive spasticity, evolving into spastic quadriplegia with opisthotonic posturing and severe multifocal contractures. Generalised tonic-clonic seizures began around age 2–2.5 years in all. All patients followed up to older ages (5–29 years) had microcephaly, severe spasticity leading to contractures, irritability and sleep disorder, as well as generalised, at times intractable, tonic clonic and myoclonic seizures accompanied by osteoporosis, progressive disabling scoliosis and short stature. Apart from the microcephaly, there were no dysmorphic features. All had profound mental retardation, gaining practically no developmental milestones except visual tracking and smiling.

While brain ultrasound in utero and MRI in the first months of life were normal, brain imaging (CT and MRI) demonstrated progressive diffuse cerebellar atrophy as early as 11 months of age, followed within a few months by cerebral atrophy. Cerebral grey and white matter atrophy accompanied by thin corpus callosum was already evident during the second year of life with further atrophic changes in follow-up studies. Detailed metabolic studies were all within normal limits, including assays in blood and fibroblasts demonstrating normal activity of a panel of lysosomal enzymes, namely: galactocerebrosidase, arylsulfatase, β galactosidase, hexosaminidase, α mannosidase, α fucosidase, as well as normal sulfatide response to cerebrosulfatide loading in fibroblasts. Serum activities of β-galactosidase, total hexosaminidase and aryl sulfatase A were within normal limits. Isoelectric focusing of transferrin was normal. Pathology analyses of skin, muscle, rectal, conjunctival and peripheral nerve biopsies were with no significant findings. Functional assays of mitochondrial complexes in muscle biopsies demonstrated normal respiratory chain activity. Cerebrospinal fluid analysis (protein, cells) was normal.

Genome-wide linkage analysis studies

Genome-wide linkage analysis (Affymetrix 10 K SNP arrays) testing all five affected individuals in families A–C and one patient of family D (figure 1A) failed to identify a homozygous genomic locus common to all affected individuals. Assuming the disease in the different families might be genetically heterogeneous, we focused on the largest kindred (Family D), conducting a more detailed genome-wide linkage analysis using 500 K SNP microarrays (subjects D-3, D-4, D-11, D-14, D-15, figure 1A). A single 500 Kb region of identical genotypes on chromosome 17p13.3 was identified, that was shared by all five patients in family D. Assuming a recessive full penetrance model, statistical analysis using SUPERLINK[6] of 25 SNPs that are 20 Kb apart on average within that locus, determined a multipoint logarithm of the odds (LOD) score of 3 for family D. Studies using polymorphic markers demonstrated that at the 500 Kb locus, affected individuals of all four kindred shared the same genotype; 2-point LOD score for all individuals of the four families was 4.98 (data not shown).

Identification of the VPS53 mutations

Whole exome sequencing of genomic DNA of affected individuals B6 and D4 was performed. After filtering the sequence data within the 500 kb region for normal variants, only three

heterozygous non-synonymous mutations were found for individual B6, and only one for individual D4: a VPS53 exon 19 c.2084A>G heterozygous mutation, that was found also in patient B6. This p.(Gln695Arg) missense mutation replaces a highly conserved amino acid in VPS53's C-terminal (figure 1B, left panel). In the whole exome sequencing data, no two mutations were found within exons of the same gene for any of the genes within the locus. However, analysis of intronic variants within the locus demonstrated that in B6 and D4, VPS53 harboured a second heterozygous mutation (figure 1B, right panel): c.1556+5G>A (NP_001121631.1; RefSeq). This mutation is in the 5th nucleotide of intron 14, and is expected to disrupt one of VPS53's splice-donor sites. Restriction analysis demonstrated complete segregation (and thus full penetrance) of both mutations with the disease-associated phenotype in all investigated individuals of the four families, with all affected individuals being compound heterozygous for the two mutations. Of Jewish Moroccan controls tested, 2:143 carried the c.2084A>G mutation and 2:156 carried the c.1556+5G>A mutation (~1:37 carrier rate for a VPS53 mutation).

RNA studies

Human Splicing Finder predicted that the VPS53 intronic mutation likely abolishes the natural splice donor site, suggesting a few dozen potential alternative splice donor sites. To delineate the novel VPS53 transcript(s) generated because of the splice site mutation, we generated cDNA from EBV-transformed lymphoblastoid cells of affected individuals and controls. PCR primer sets were designed to specifically amplify transcripts harbouring the splice-site c.1556+5G>A mutation and not the other allele, as the expected amplicons extended into intron 14: forward primer (from within exon 13) was GCCTCATCTCTACGTGTATATCG. Reverse primers were selected at growing intervals from within intron 14 (primer sequences available upon request). The largest amplicon generated extended 781 bp into intron 14 (reverse primer CGGGTTCAAGTGATTCTC). As expected for this primer set, the PCR amplification reaction done on patient D11's cDNA generated the mutant c.1556+5G>A allele only (figure 1B, right panel).

Sequencing of exon 19 of VPS53 from cDNA of affected individuals demonstrated only the c.2084A>G missense mutation and not the wild-type sequence expected at that position in the other allele (figure 1B, left panel). Quantitative RT-PCR amplification of exons 19–20 from affected individuals using a primer set (A) specific to the wild-type sequence barely generated any amplification (figure 2E), while a primer set (B) specific to the exon 19 missense mutation sequence generated effective amplification from the same cDNAs (figure 2F). Furthermore, quantitative RT-PCR amplifying exons 15–16 demonstrated a ~twofold reduction in mRNA levels of the C terminal of VPS53 in lymphoblastoid cells of affected individuals compared with controls (figure 2D). These findings suggested that in cells of affected individuals, the VPS53 allele that harbours the c.1556+5G>A splice site mutation might be unstable, possibly undergoing nonsense-mediated mRNA decay. However, sequencing of natural variant rs11558129 within exon 1 of VPS53 from cDNA of affected individuals demonstrated heterozygosity (figure 1C); moreover, we could amplify the splice site mutant allele from cDNA of cells of affected individuals. Thus, the data are more consistent with an abnormal structure of the mRNA beyond intron 14, lacking part or all of exons 15–16 and 19–20. It should be noted that the transcript bearing the c.1556+5G>A splice site mutation extends into intron 14 (figure 2H), reaching a premature stop codon immediately after the last
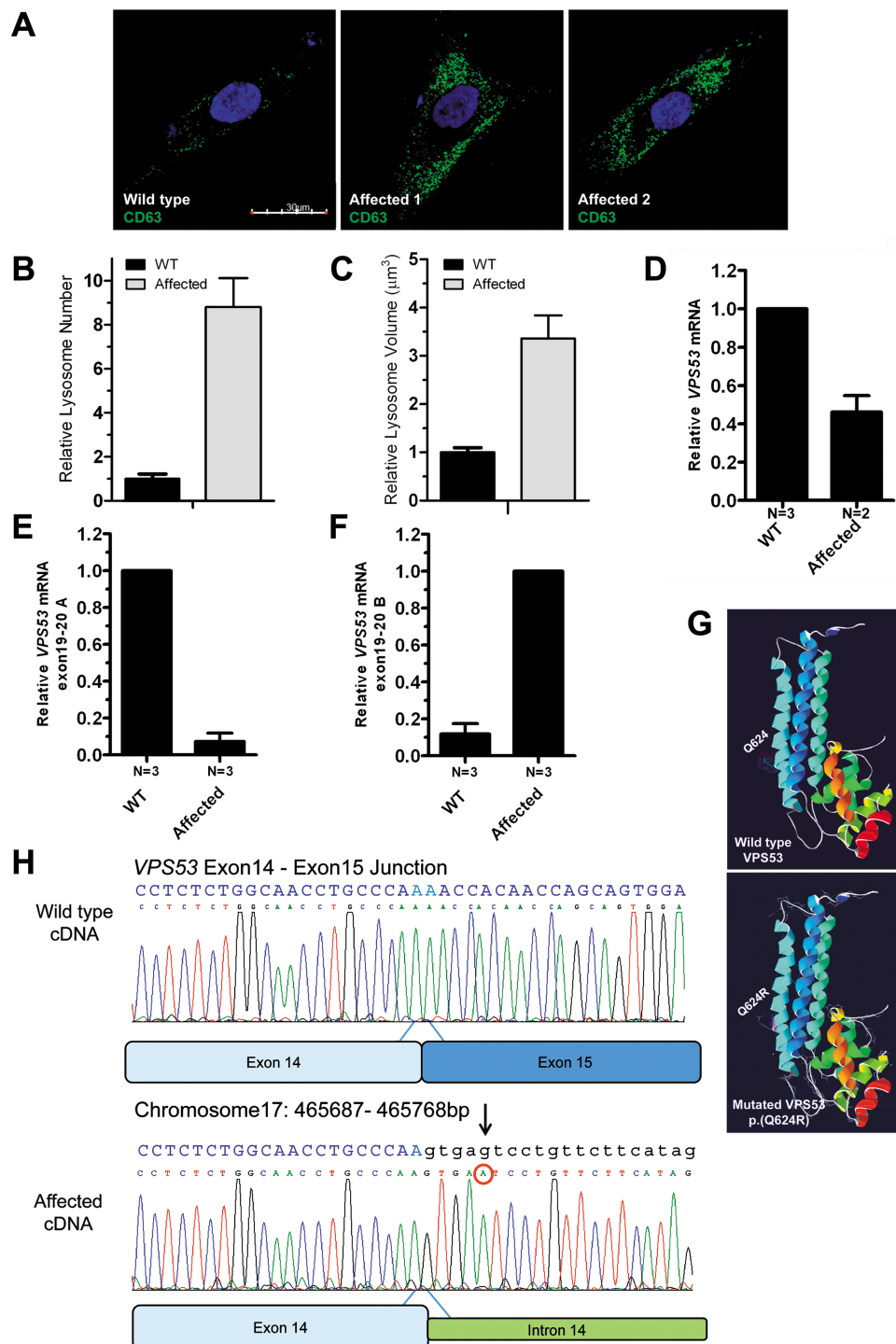
Figure 2 Phenotypic and molecular consequences of *VPS53* compound mutations. (A) Affected individuals' fibroblasts show accumulation of swollen CD63-positive structures; cells were labelled with an antibody to CD63 (green channel), followed by secondary antibodies. DAPI blue channel, scale=30 μm. Affected individuals' cells (affected 1 and 2) show marked abundance of swollen CD63-stained MVBs relative to the controls. (B and C) Image analysis (Volocity software) demonstrating that number (8-fold) and volume (3-fold) of CD63-positive MVBs was higher (p<0.0001 per t test) in fibroblasts of affected individuals (grey bars) versus controls (black bars). Objects <0.5 μm, not likely to be MVBs, were excluded. Data (mean±SEM) represent 3 separate experiments, each testing 2 controls and 2 affecteds, 5 different cells per individual. (D) Relative *VPS53* mRNA levels in Epstein–Barr virus (EBV) transformed lymphoblastoid cell lines of controls versus affected individuals (mean±SD, n=2). *GAPDH* used as control. (E and F) Relative *VPS53* mRNA levels of amplicons generated using PCR primer set A, specific to the wild-type exon 19–20 sequence (E), or primer set B, specific to the c.2084A>G mutated exon 19–20 sequence (F) in cells of controls versus affected individuals (mean±SD, n=3). *GAPDH* used as control. (G) SPDBV ribbons diagram of tertiary structure of Yeast VPS53. The p.(Q695R) mutation in the equivalent yeast position p.(Q624R) shown in pink. (H) Sequencing of affected individual's cDNA presenting an intronic sequence (rather than exon 15 sequence) following exon 14.

amino acid encoded by exon14 (ExPaSy translation tool). Thus, any transcripts containing the splice-site mutation are expected to encode a truncated protein, making any cryptic splice-donor-sites within intron 14 irrelevant to the final protein sequence.

Immunofluorescence microscopy studies

To examine possible functional consequences of the compound heterozygous mutations in our patients, we performed immuno-fluorescence microscopy studies of fibroblast cell lines. In fibroblasts of affected individuals, CD63-positive vesicles appeared swollen and numerous relative to control cells (figure 2A–C). This finding was consistent in all three triplicate experiments in cell lines of two affected individuals (D3 and D11, figure 1A) and two controls.

DISCUSSION

The Golgi-associated retrograde protein (GARP) consists of four subunits: Ang2, Vps52, Vps53 and Vps54, that form an obligatory 1:1:1:1 complex. GARP is localised to the trans-Golgi network (TGN), where it functions as a tethering factor for retrograde transport carriers that recycle lysosomal sorting receptors from endosomes to the TGN.[7–10] Depletion of GARP subunits by RNAi in human cells precludes fusion of retrograde transport carriers with the TGN, blocking the recycling of lysosomal sorting receptors and eventually leading to missorting of their cargo lysosomal hydrolases to the extracellular space. As a consequence, lysosomes become swollen, likely due to a buildup of undegraded materials.[7 10]

GARP-SNARE interactions are necessary to promote retrograde transport to the TGN, with possible involvement of GARP in tethering by recognition of factors other than SNAREs through the C-terminal domain of Vps53.[11] VPS53's C-terminal consists of two α-helical bundles arranged in tandem with a highly conserved surface patch, likely to play a role in vesicle recognition: the structure of the C-terminal fragment of the Vps53 subunit is important for binding endosome-derived vesicles, and mutations of the surface patch region result in defects in membrane trafficking.[12] In fact, deletion of the C-terminal region of Vps53 was shown to disrupt GARP's tethering role.[11]

The c.2084A>G p.(Gln695Arg) mutation replaces a neutral amino acid with a positively charged one within the second helix of the surface of Vps53's conserved C-terminal, in one of the most conserved positions of the molecule (figures 1B and 2G).[12] The c.1556+5G>A splice site mutation generates an aberrant/unstable transcript that is predicted to encode a truncated protein, leaving the affected individuals with no functional VPS53 C-terminus and partially dysfunctional GARP. GARP complex interactions with vesicles, as part of the evacuation of cellular waste in the lysosome, depend on VPS53's C-terminal integrity.[7 11 12] CD63 is known to be located primarily in the inner leaflet of the late endosomes, though it can be found also in multivesicular bodies (MVB), in some early endosomes, and in the lysosomal membrane.[13] Our data demonstrate abundance and swelling of CD63 positive vesicles in fibroblasts of affected individuals. It has been previously shown that GARP defects may lead to missorting of the lysosomal hydrolases to the extracellular space. While our CD63 immunostaining data together with the known roles of the GARP complex could imply that the VPS53 mutations cause a lysosomal disease, none of the patients had typical features of a lysosomal storage disorder, such as progressive leukodystrophy, abnormal activity of lysosomal enzymes in cells or sera, or evidence of a storage disorder in rectal, conjuctival, muscle, skin or peripheral nerve biopsies. Thus, it is plausible that the PCCA phenotype in the affected

patients is due to abrogation of other, non-lysosomal-associated functions of VPS53. In fact, the function of GARP at the TGN is not limited to recycling of lysosomal sorting receptors but is also required for other functions, such as retrograde transport of other recycling proteins, such as the human TGN46 and B-subunit of Shiga toxin.[7] This is in line with the CD63 staining, suggesting that the multiple swollen vesicles in affected fibroblasts are likely to be transport intermediates/late endosomes.[11] The precise mechanism by which the VPS53 mutations lead to PCCA is yet unclear.

Possibly pathogenic mutations in VPS54, encoding another protein of the GARP complex, have been associated with human amyotrophic lateral sclerosis (ALS). Moreover, 'wobbler' mice bearing a hypomorphic missense substitution in Vps54 serve as a model of ALS, while homozygous null mutant Vps54 mice die in utero.[14 15] Thus, functional insights as to the emergence of different phenotypes secondary to mutations in different members of the GARP complex, are yet to be elucidated.

Finally, with a carrier rate of ∼1:37 of VPS53 mutations in Jews of Moroccan ancestry, routine carrier screening for these mutations in this large community should be considered. Furthermore, VPS53 mutations should be sought in cases of PCCA worldwide.

WEB RESOURCES

The URLs for data presented herein are as follows:
ConSeq server: http://consurf.tau.ac.il/
UCSC: Genome browser: http://genome.ucsc.edu/cgi-bin/hgGateway
Chromas: http://www.technelysium.com.au/chromas.html
HaploPainter: http://haplopainter.sourceforge.net/index.html
MarshfieldMaps: http://research.marshfieldclinic.org/genetics/GeneticResearch/compMaps.asp
New England Biolabs NEBcutter (V.2.0): http://tools.neb.com/NEBcutter2/
Online Mendelian Inheritance in Man (OMIM): http://www.ncbi.nlm.nih.gov/Omim/
Primer3 (V.0.4.0): http://frodo.wi.mit.edu/primer3/
Simple Modular Architecture Research Tool (SMART): http://smart.embl-heidelberg.de/
SUPERLINK: http://bioinfo.cs.technion.ac.il/superlink-online.gridbot/makeped/MultiPointAnalys.html
SNP database: http://www.ncbi.nlm.nih.gov/projects/SNP/
Exome Variant Server, NHLBI: http://evs.gs.washington.edu/EVS/
ExPaSy: DeepView—Swiss-PdbViewer: http://spdbv.vital-it.ch/disclaim.html
ExPaSy Translate tool: http://web.expasy.org/translate/
1000 Genome Database: http://www.1000genomes.org/
RefSeq: http://www.ncbi.nlm.nih.gov/refseq/
Berkeley Drosophila Genome Project: http://www.fruitfly.org/seq_tools/splice.html
Human Splicing Finder: http://www.umd.be/HSF/

REFERENCES

1 Ben-Zeev B, Hoffman C, Lev D, Watemberg N, Malinger G, Brand N, Lerman-Sagie T. Progressive cerebellocerebral atrophy: a new syndrome with microcephaly, mental retardation, and spastic quadriplegia. *J Med Genet* 2003;40:e96.

2 Agamy O, Ben Zeev B, Lev D, Marcus B, Fine D, Su D, Narkis G, Ofir R, Hoffmann C, Leshinsky-Silver E, Flusser H, Sivan S, Soll D, Lerman-Sagie T, Birk OS. Mutations disrupting Selenocysteine formation cause progressive cerebello-cerebral atrophy. *Am J Hum Genet* 2010;87:538–44.

3 Markus B, Narkis G, Landau D, Birk RZ, Cohen I, Birk OS. Autosomal recessive congenital contractural syndrome type4 (LCCS4) caused by a mutation in MYBPC1. *Hum Mut* 2012;33:1435–8.

4 Cohen I, Birnbaum RY, Leibson K, Taube R, Sivan S, Birk OS. ZNF750 is expressed in differentiated keratinocytes and regulates epidermal late differentiation genes. *PLoS ONE* 2012;7:e42628.

5 Nishimura R, Ushiyama A, Sekiguchi S, Fujimori K, Ohuchi N, Satomi S, Goto M. Effects of glucagon-like Peptide 1 analogue on the early phase of revascularization of transplanted pancreatic islets in a subcutaneous site. *Transpl Proc* 2013;45:1892–94.

6 Silberstein M, Tzemach A, Dovgolevsky N, Fishelson M, Schuster A, Geiger D. Online system for faster multipoint linkage analysis via parallel execution on thousands of personal computers. *Am J Hum Genet* 2006;78:922–35.

7 Conibear E, Stevens TH. Vps52p, Vps53p, and Vps54p form a novel multisubunit complex required for protein sorting at the yeast late Golgi. *Mol Biol Cell* 2000;11:305–23.

8 Conibear E, Cleck JN, Stevens TH. Vps51p mediates the association of the GARP (Vps52/53/54) complex with the late Golgi t-SNARE Tlg1p. *Mol Biol Cell* 2003;14:1610–23.

9 Siniossoglou S, Pelham HR. An effector of Ypt6p binds theSNARE Tlg1p and mediates selective fusion of vesicles with late Golgi membranes. *EMBO J* 2001;20:5991–8.

10 Pérez-Victoria FJ, Mardones GA, Bonifacino JS. Requirement of the human GARP complex for mannose 6-phosphate-receptordependent sorting of cathepsin D to lysosomes. *Mol Biol Cell* 2008;19:2350–62.

11 Pérez-Victoria FJ, Bonifacino JS. Dual roles of the mammalian GARP complex in tethering and SNARE complex assembly at the trans-golgi network. *Mol Cell Biol* 2009;29:5251–63.

12 Vasan N, Hutagalung A, Novick P, Reinisch KM. Structure of a C-terminal fragment of its Vps53 subunit suggests similarity of Golgi-associated retrograde protein (GARP) complex to a family of tethering complexes. *Proc Natl Acad Sci USA* 2010;107:14176–81.

13 Kobayashi T, Vischer UM, Rosnoblet C, Lbrand C, Lindsay M, Parton RG, Kruithof EKO, Gruenberg J. The Tetraspanin CD63/lamp3 cycles between endocytic and secretory compartments in human endothelial cells. *Mol Biol Cell* 2000;11:1829–43.

14 Schmitt-John T, Drepper C, Mussmann A, Hahn P, Kuhlmann M, Thiel C, Hafner M, Lengeling A, Heimann P, Jones JM, Meisler MH, Jockusch H. Mutation of Vps54 causes motor neuron disease and defective spermiogenesis in the wobbler mouse. *Nat Genet* 2005;37:1213–15.

15 Pérez-Victoria FJ, Schindler C, Magadán JG, Mardones GA, Delevoye C, Romao M, Raposo G, Bonifacino JS. Ang2/fat-free is a conserved subunit of the Golgi-associated retrograde protein complex. *Mol Biol Cell* 2010;21:3386–95.

VPS53 mutations cause progressive cerebello-cerebral atrophy type 2 (PCCA2)

Miora Feinstein, Hagit Flusser, Tally Lerman-Sagie, et al.

Updated information and services can be found at:

http://jmg.bmj.com/content/early/2014/02/27/jmedgenet-2013-101823.full.html

These include:

References	This article cites 15 articles, 9 of which can be accessed free at: http://jmg.bmj.com/content/early/2014/02/27/jmedgenet-2013-101823.full.html#ref-list-1
P<P	Published online February 27, 2014 in advance of the print journal.
Email alerting service	Receive free email alerts when new articles cite this article. Sign up in the box at the top right corner of the online article.

Topic Collections	Articles on similar topics can be found in the following collections Clinical diagnostic tests (330 articles) Immunology (including allergy) (529 articles) Epilepsy and seizures (162 articles) Genetic screening / counselling (783 articles)

Notes

Advance online articles have been peer reviewed, accepted for publication, edited and typeset, but have not not yet appeared in the paper journal. Advance online articles are citable and establish publication priority; they are indexed by PubMed from initial publication. Citations to Advance online articles must include the digital object identifier (DOIs) and date of initial publication.